X-ray microscopy of beryllium

1960 Br. J. Appl. Phys. 11 498

(http://iopscience.iop.org/0508-3443/11/11/304)

(7) KENTY, C. *Phys. Rev.*, **80**, p. 95 (1950).
(8) SPENKE, E. *Z. Phys.*, **127**, p. 221 (1950); see also Ref. (4), p. 128.
(9) KENTY, C. *Phys. Rev.*, **42**, p. 823 (1932).
(10) HOLSTEIN, T. *Phys. Rev.*, **72**, p. 1212 (1947); **83**, p. 416 (1951).
(11) FOWLER, R. G. *Handb. Phys.*, **22**, p. 209 (Berlin: Springer-Verlag, 1956).
(12) EASELY, M. A. *J. Appl. Phys.*, **22**, p. 590 (1951).
(13) CAYLESS, M. A. *Brit. J. Appl. Phys.*, **10**, p. 186 (1959).
(14) CAYLESS, M. A. *The Computer Journal.* To be published.

X-ray microscopy of beryllium

by J. SAWKILL, M.Met., Ph.D., and D. R. SCHWARZENBERGER, B.A., Tube Investments Research Laboratories Hinxton Hall, Cambridge

[*Paper received* 6 *July*, 1960]

Abstract

The point-projection X-ray microscope has been used to study a variety of beryllium specimens, ranging from single crystals to finely-polycrystalline metal containing inclusions. The highly divergent beam of X-rays from a source 1 μ *in diameter gives, on the same photograph, a microradiograph of the specimen with a resolution of* 1 μ *and a divergent beam diffraction pattern. Together these can give information about the distribution of heavier elements or cracks in the beryllium, the variation in perfection of the crystal lattice and, with a single crystal, the orientation and lattice parameters of the specimen.*

Introduction

THE point-projection X-ray microscope[1] provides a highly divergent beam of X-rays from a source about 1 μ in diameter, suitable for both microradiography and divergent beam X-ray diffraction. A diagram of the experimental arrangement is given in Fig. 1. The electron beam is focused on to a metal foil about 1μ thick, which

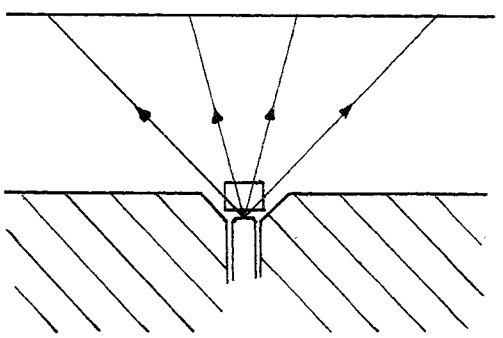

Fig. 1. Experimental arrangement of the X-ray microscope

acts as a transmission target. The specimen is placed in air immediately above the target, giving a shadow on the fluorescent screen or photographic plate placed in the path of the transmitted beam. The magnification is given by the ratio of the distance between the target and screen, to the distance between the target and specimen. The high primary magnification allows visual inspection of larger inclusions and the location of areas of particular interest. As the source of X-rays is very small, the depth of focus is large, so that the specimen may be at any position between the target and plate according to the magnification required; a thick specimen of any shape can be observed, although the magnification then varies considerably throughout the specimen thickness. Normally no special preparation of the specimen is required.

If the accelerating voltage, which may be varied between 15 and 50 kV, is above the excitation voltage for the characteristic X-rays of the particular target in use, a transmission divergent beam diffraction pattern may be recorded from a crystalline specimen, in addition to the shadow microradiograph. Published work describing the use of the point-projection X-ray microscope for the examination of metallurgical specimens concentrates almost entirely on the microradiograph [see, for example, the articles in Ref. (2)], while the diffraction effects occurring in a divergent beam have generally been used for observations on the perfection and lattice parameters of good single crystals only [e.g. as in Ref. (3)]. Many metallurgical specimens, including most of the beryllium specimens studied, give rise to both types of contrast so that a transmission divergent beam diffraction pattern is superimposed on the microradiograph. Consideration of the two together often gives additional information about the microstructure of a specimen. Contact microradiographs of some thin beryllium specimens have been given by Udy,[4] but this arrangement shows no diffraction contrast.

Beryllium is particularly suitable for microradiographic examination because of its low absorption coefficient for X-rays; the presence of most heavier elements is shown up by a large decrease in the transmitted intensity. The exposure times for beryllium specimens up to 1 cm in thickness were about fifteen seconds with the photographic plate 4 cm above the X-ray source, using Ilford Special Lantern Contrasty Emulsion.

Absorption contrast

As the absorption coefficients of most other elements are much greater than that of beryllium, small amounts of other elements in solution may be expected to decrease the transmitted X-ray intensity considerably. For example, for a beryllium specimen 0·6 cm in thickness, the addition of 0·1% by weight of iron decreases the transmitted X-ray intensity to 73% of its original value (calculated for CuKα radiation,

neglecting fluorescence). In addition, most elements have a very small solid solubility in beryllium, so that even small amounts of impurity or alloying elements are likely to be present as a second phase, giving an even greater contrast against the beryllium matrix than if dispersed in a solid solution.

Figs. 2 to 5 are photographs of specimens of beryllium with a heavier second phase present, giving good contrast by the difference in absorption coefficient. Figs. 2 and 3 are microradiographs of extruded beryllium with heavier included material; the specimen was in the form of a cylinder, 1 cm in diameter and 0·5 cm in length parallel to the extrusion direction. The length was placed normal to the photographic plate for Fig. 2 and parallel to it for Fig. 3. The magnification on the print varies between about ten times for the part nearest the X-ray source to five times for the furthest part of the specimen. With the arrangement as in Fig. 1, vertical features in the specimen appear radial on the photograph as well as the truly radial features. These can be distinguished by taking stereoscopic pairs of photographs, or two photographs at right angles, as in Figs. 2 and 3. Comparison of these photographs shows that the large inclusions are, in fact, alined parallel to the extrusion direction. The grain size in a transverse section was about 0·002 cm, which is too small for any distinct diffraction contrast to be seen. [See paragraph (iii) under Diffraction contrast.]

Fig. 4 is a microradiograph of a sintered alloy of beryllium with 5% ruthenium. In the region shown, the specimen thickness is two or three times the grain diameter. The ruthenium rich phase is present in a needle-like structure, apparently in grain boundary regions, and the same structure was observed in an optical examination. Fig. 5 is a microradiograph of a rolled sheet, 0·01 cm thick, of an alloy of beryllium with 1·8% silicon. The silicon rich phase is in particles which appear to be distributed at random in the matrix, but observations on stereoscopic pairs of photographs showed that the particles were in strings parallel to the rolling direction. Several other alloys of beryllium with small amounts of other materials were examined; the heavier the alloying element, the greater the contrast. In general, the second phase was continuous in grain boundary regions in the sintered alloys, but broken up into discrete particles in the rolled sheet alloys.

Diffraction contrast

(i) *Single crystal.* When a highly divergent beam of X-rays is transmitted through a single crystal, diffraction leads to a pattern of cones of deficient and excess intensity (Fig. 6); (hkl) planes of spacing d give rise to a deficient cone of angular radius $\cos^{-1}(\lambda/2d)$, and axis [*hkl*]. The expected pattern of deficiency cones can thus be calculated for a given X-ray wavelength and crystal structure, and drawn (e.g. on a stereographic projection) for comparison with the conic sections recorded on the photographic plate. This allows the deficiency conics to be indexed and the approximate orientation of the crystal to be seen. It was found that for a beryllium single crystal, giving sufficient contrast for the deficiency conics to be visible on a fluorescent screen, the orientation could be seen directly when a prominent crystallographic axis was approximately normal to the screen [e.g. $[10\bar{1}0]$ as in Fig. 7]. The pattern of excess conics depends on the relative positions of the specimen, source and plate, in addition to the crystal structure and the X-ray wavelength, while the deficiency line pattern is independent of the exact experimental arrangement.

Observations on the deficiency line pattern may allow the lattice parameters to be calculated in terms of the wavelength only. An intersection of three or more conics at a single point may arise from the symmetry of the lattice and be independent of the wavelength; for example, in any cubic crystal the deficiency conics from (200) and (020) planes always intersect on the conic from the (220) planes. Other multiple intersections, however, may depend on the relation between the X-ray wavelength and the lattice parameters of the crystal. Then, under favourable circumstances, calculations from such exact or near coincidences may allow the lattice parameters to be determined accurately for crystals of high symmetry. Calculations from two such coincidences, exact for $CuK\alpha_2$ radiation, on a photograph of a beryllium crystal taken on the point-projection X-ray microscope, gave

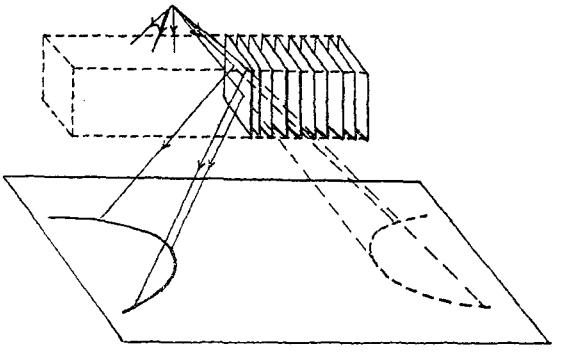

Fig. 6. Diagrammatic representation of the formation of deficiency and reflexion conics

the following values for the lattice parameters: $a = 2{\cdot}2866 \pm 0{\cdot}0006$ Å, $c = 3{\cdot}5833 \pm 0{\cdot}0009$ Å, $c/a = 1{\cdot}5671$, at at 22° C.[5] With cubic crystals of greater perfection, lattice parameters have been determined with an accuracy of $\pm 0{\cdot}002\%$,[3] compared with $\pm 0{\cdot}026\%$ for the beryllium values quoted here.

(ii) *Imperfections.* If the crystal is perfect, the deficiency lines are very narrow and may be difficult to record on a photograph, whereas with a less perfect or strained crystal, the lines are broadened. When there is a continuous variation in orientation within a single crystal the lines may be very wavy, and the presence of subgrains gives rise to deficiency conics with several distinct components. The angular orientation differences present in the crystal may be estimated by comparison of the distances on the photographic plate, between the components of a conic arising from the substructure, and from the known Kα doublet separation for the particular radiation and set of reflecting planes. For example, the (0002) lattice spacing of beryllium is 1·79 Å, the $CuK\alpha_1$ and α_2 wavelengths are approximately 1·540 and 1·544 Å, giving a difference in the angular radius of the (0002) deficiency cone of 4′ of arc. Then, if the components arising from differently oriented regions within the crystal are sharp lines, angular differences down to about 2′ of arc may be detected. The direction in which the lattice is rotated, in passing across a low-angle boundary, may be estimated by a comparison of the extent and direction of the splitting of different conics. This may not detect all subgrains in the crystal, as the whole volume of the crystal is not observed at once, but only those parts which are on the surfaces of the cones from which diffraction occurs.

(iii) *Polycrystalline specimens.* With a polycrystalline specimen, short lengths of deficiency lines are recorded and

not a complete pattern of conics (compare Figs. 7 and 9), as directions deficient in X-rays can occur only within the projection of the grain in which they arise. In general, indices cannot be assigned to the lines, and only a qualitative estimate of the substructure and perfection can be made. For a grain of diameter D and magnification on the plate M, the maximum length of a section of a deficiency conic recorded on the plate is DM; the length s of the recorded section of a deficiency conic is usually less than this, as the line does not necessarily coincide with the grain diameter; indeed, the orientation of some grains may prevent entirely the occurrence of deficiency lines in their projected area. If the grains are very small, the sections of deficiency conics may be so short and close together that they cannot easily be distinguished. To estimate the minimum grain diameter required for the deficiency lines to be visible, the effective width w of a deficiency line may be taken as approximately the Kα doublet separation in the plane of the plate, and the line assumed to be distinguishable if $s > 4w$; i.e. for a single layer of grains $D > 4w$. For n layers of grains, one above another, the patterns overlap; if the grains are approximately spherical, and the deficiency lines are assumed to be visible if they occupy the same proportion of total area as for a single layer, the minimum grain diameter is $4nw$. The specimen thickness $t = nD$, giving the minimum grain diameter at which some diffraction contrast is recognizable as $4wt$. This estimate is probably rather low, and should be increased to allow for the sections of deficiency lines not always coinciding with the maximum diameter of a grain. It should also be increased if the lines are broadened by the crystal imperfections, or if the lattice parameters are large, compared with the wavelength of the radiation, so that even for a single crystal there are many reflexions. Using this criterion, the calculated minimum grain diameter at which the deficiency lines may be distinguished, for a specimen of beryllium 0·1 cm thick at 0·5 cm above a copper target, is about 0·001 cm, taking an average value of w for all possible reflexions. There is, however, an additional factor to consider: a single crystal or an individual grain in a polycrystalline specimen must be of a suitable thickness in the direction of the incident X-ray beam for deficiency conics of reasonable contrast to occur. For beryllium, with such a low absorption coefficient for X-rays, the minimum thickness is as great as 0·02 cm, so that this criterion, rather than length and overlapping of deficiency line sections, governs the minimum grain diameter for observation of diffraction contrast.

Combined microradiograph and diffraction pattern

Microradiographs of beryllium specimens with large variations in X-ray absorption, but no appreciable diffraction contrast, and the deficiency line pattern arising from diffraction in a specimen of uniform absorption coefficient, have been considered in the previous sections. Most specimens are intermediate between these two extremes, and a deficiency line pattern is recorded simultaneously with the microradiograph.

There are several advantages in considering these two types of information together. The deficiency line pattern is of value in revealing the grain-size of the specimen when the microradiograph shows inclusions in the material, showing whether they are concentrated at the grain boundaries or within the grains. Similarly, transgranular and intergranular cracking can be distinguished. In the deformation and recrystallization of a specimen, as described in more detail in paragraph (ii) below, the changing perfection of the grains can be followed and correlated with the development of cracks or the positions of inclusions, as seen by absorption contrast. The short exposure time is an added advantage, allowing continuous changes, for example during the recrystallization of a specimen, to be followed by a series of photographs at short intervals of time. Precipitation effects in an alloy might similarly be followed by differences in absorption in the microradiograph, while any change in lattice parameter or perfection could be detected at the same time.

Two beryllium specimens giving a deficiency line pattern with the microradiograph have been studied in detail.

(i) Photographs have been taken at intervals along a zone-refined single-crystal rod of beryllium, about 25 cm in length and 0·6 cm in diameter, with the impurities concentrated towards one end by the zone refining process. At the pure end, Fig. 7, the pattern of deficiency conics is sharp, with no subgrains in the crystal, and no absorption contrast from the presence of heavier elements. By comparison with a stereographic projection of the expected pattern of conics, the orientation can be seen to be [10$\bar{1}$0] normal to the photograph, with [11$\bar{2}$0] approximately along the length of the rod, from left to right on the photograph, i.e. basal planes are parallel to the length of the rod. After this highly perfect region, about 1 cm in length, the conics become split into several sharp components; almong most of the crystal there are three main components, corresponding to a total range of orientation of just under 1°. The directions of the orientation differences indicate that the subgrains are columnar, parallel to the length of the rod. At 18 cm from the pure end, precipitated impurity particles are first seen. The impurity appears to be concentrated in bands, rather than increasing smoothly from a low concentration at one end to a high concentration at the other. Fig. 8 shows such a discontinuity in the concentration of impurity, probably arising from a decrease in the volume of the molten zone during refining. The rod remains essentially a single crystal with fairly sharp deficiency conics and a range of orientation not greater than about 1°, even where the concentration of impurity is very high. Two photographs gave sufficiently clear deficiency line patterns, with suitable multiple intersections in Cu$K\alpha_2$ radiation, to allow the lattice parameters to be determined in terms of the wavelength. In a fairly clear region, at about 20 cm from the pure end of the crystal, the coincidences appeared exact, giving the values of a and c quoted in the section on Diffraction contrast. At the pure end, Fig. 7, the radii of the conics are slightly smaller, indicating a decrease of 0·02% in a and c, assuming c/a, and hence the absolute values of a and c separately could not be determined. This indicates that impurities expand the lattice slightly.

Thus a single series of photographs taken at intervals along the rod gives information about the variation in perfection, the variation in lattice parameters and the distribution of impurities in the crystal.

(ii) The deformation and recrystallization of a polycrystalline specimen of cast beryllium has been followed by divergent beam X-ray photography. The specimen was a cylinder 1 cm in diameter and 0·5 cm in thickness, with a grain size of about 0·1 cm. In the as-cast state, Fig. 9(*a*), the pattern consists of short sections of deficiency conics, with overlapping from the presence of several grains in the thickness of the specimen; the presence of subgrains gives rise to lines split into several components, and strains broaden the lines so that the Kα doublet is not resolved in all the grains.

After 2% compression of the specimen at room temperature,

the lines are broader and more wavy from distortions in the crystal lattice, Fig. 9(*b*). With further compression this effect increases and cracks develop, until after 10% compression, as in Fig. 9(*c*), the deficiency lines can scarcely be distinguished and extensive cracking is observed. After recrystallization of the specimen at 950 C for two hours, Fig. 9(*d*) shows that the cracks are still present, although a sharp deficiency line pattern has returned. The lines are now split solely from the Kα doublet separation, indicating the absence of subgrains, and are slightly shorter, showing that the grain size has decreased. Porosity and cracking are difficult to observe in beryllium purely by absorption contrast, as the absorption coefficient of beryllium does not differ greatly from that of air. This is, however, partially offset by the occurrence of total external reflexion of X-rays incident at a glancing angle on an internal air-beryllium surface, outlining cracks with bright and dark lines. The refractive index for FeKα radiation in beryllium is $1 - 5 \cdot 10^{-6}$, giving a critical glancing angle of 10′ of arc up to which total external reflexion can occur. Thus the reflected X-rays suffer a deviation of a few minutes of arc only, and the resulting crack outline is only slightly displaced or distorted compared with the microradiograph. Total external reflexion of X-rays is particularly noticeable for specimens of low X-ray absorption.

Acknowledgements

The single-crystal specimens of beryllium were kindly provided by the Atomic Weapons Research Establishment, Aldermaston, and the alloys by the Atomic Energy Research Establishment, Harwell, and the Brush Beryllium Co. We should like to thank Dr. J. W. Menter for valuable discussions, and the Chairman of Tube Investments Ltd. for permission to publish this work.

References

(1) COSSLETT, V. E., and NIXON, W. C. *Proc. Roy. Soc. B*, **140**, p. 422 (1952).

(2) COSSLETT, V. E., ENGSTRÖM, A., and PATTEE, H. H. *X-ray Microscopy and Microradiography* (New York: Academic Press Inc., 1957).

(3) LONSDALE, K. *Phil. Trans Roy. Soc.*, **240**, p. 219 (1947).

(4) UDY, M. C. *The Metal Beryllium*, Chapter 8, p. 515 (Cleveland: American Society of Metals, 1955).

(5) SCHWARZENBERGER, D. R. *Phil. Mag.*, **4**, p. 1242 (1959).

X-ray microscopy of beryllium microradiographs, Figs. 2–5, 7–9

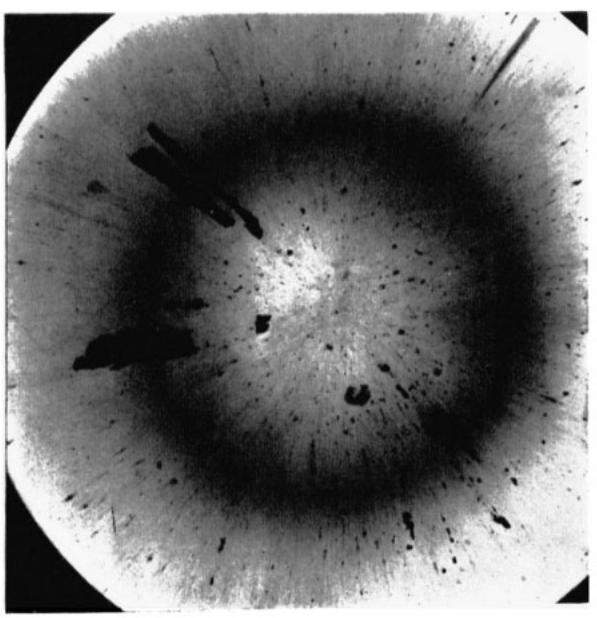

Fig. 2. Extruded beryllium with heavy included material. Copper radiation. Magnification · 5 to · 10

Fig. 3. Extruded beryllium with heavy included material. Copper radiation. Magnification · 1½ to · 10

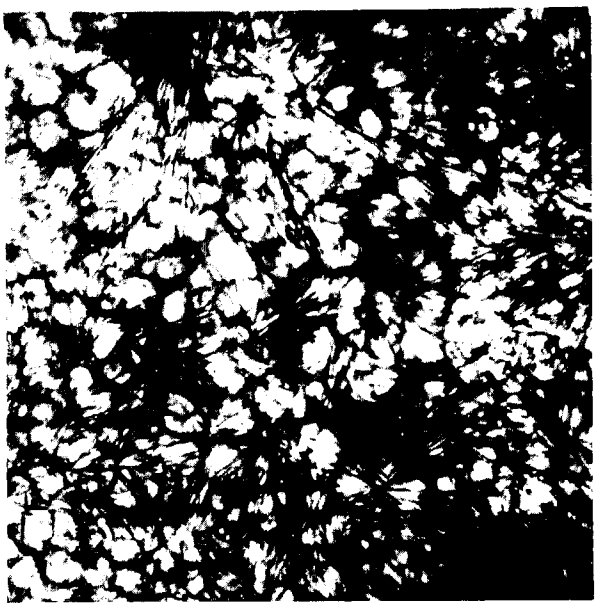

Fig. 4. Sintered alloy beryllium 5% ruthenium. Copper radiation. Magnification 75

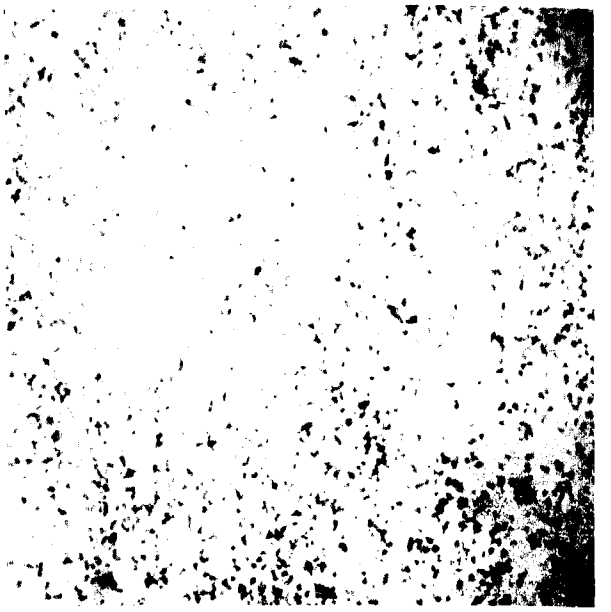

Fig. 5. Rolled alloy sheet beryllium 1·8% silicon. Copper radiation. Magnification 75

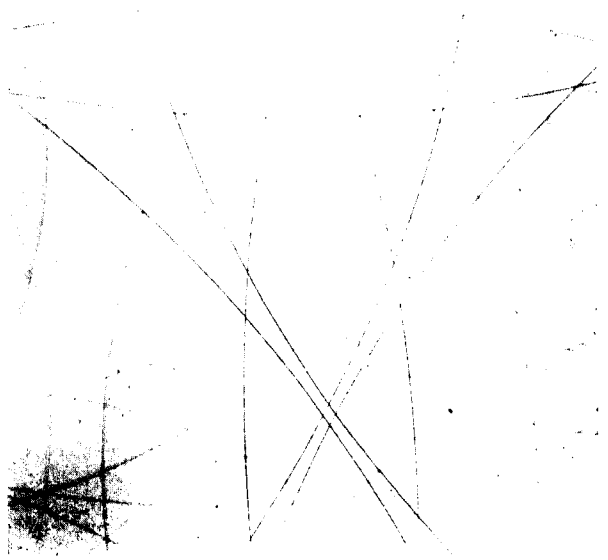

Fig. 7. Pure end of a zone-refined crystal of beryllium. Copper radiation. Magnification 20

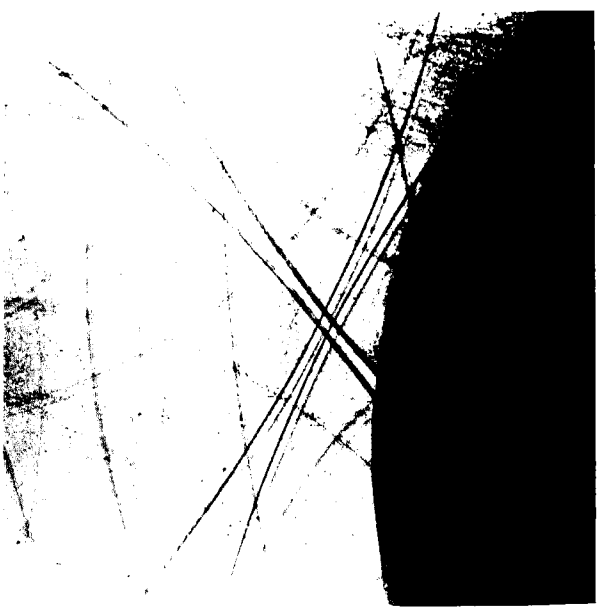

Fig. 8. Impure end of a zone-refined crystal of beryllium. Copper radiation. Magnification 20

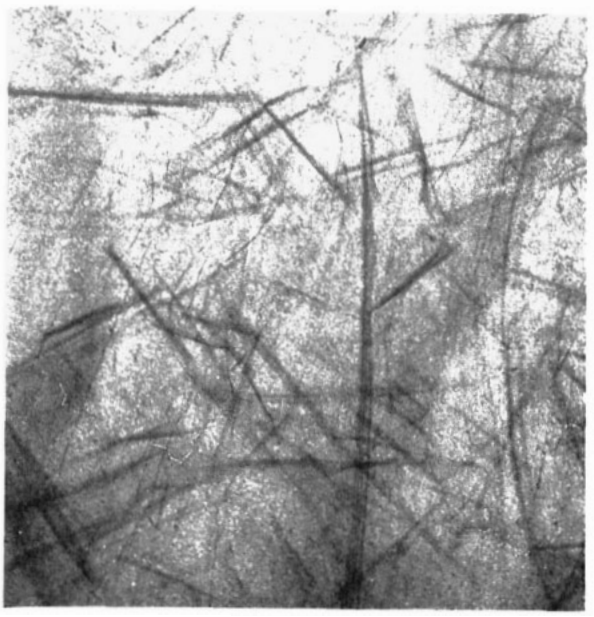

Fig. 9(*a*). Polycrystalline beryllium as cast. Iron radiation. Magnification · 10 to · 25

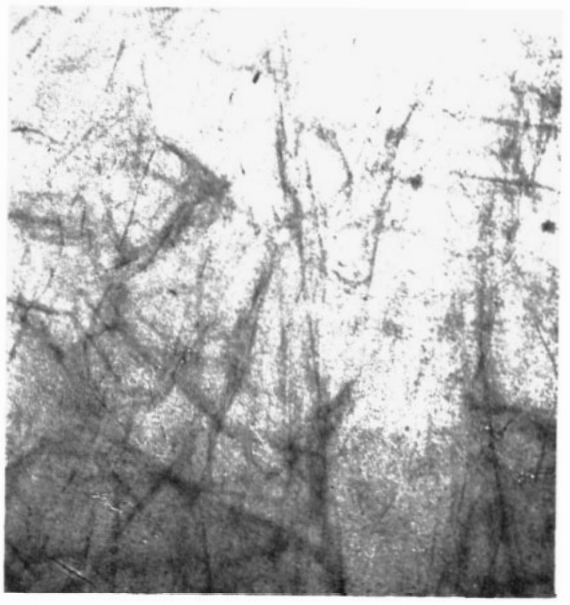

Fig. 9(*b*). Polycrystalline beryllium after 2% compression

Fig. 9(*c*). Polycrystalline beryllium after 10% compression

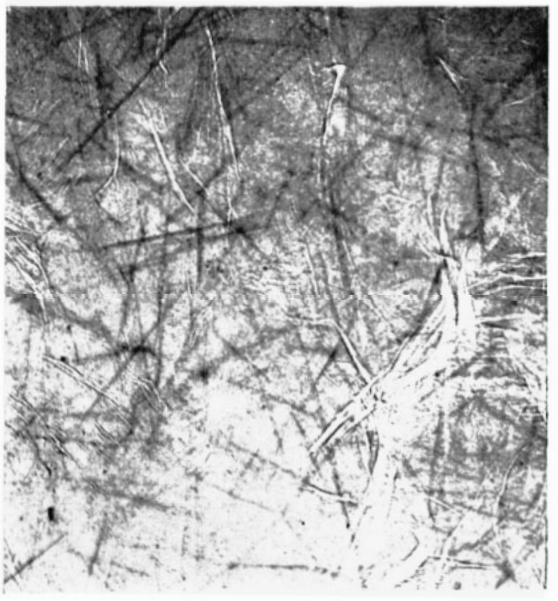

Fig. 9(*d*). Polycrystalline beryllium recrystallized